Macroscopically ordered state in exciton system

L. V. Butov[1,2], A. C. Gossard[3], and D. S. Chemla[1,4]

[1]*Materials Sciences Division, E. O. Lawrence Berkeley National Laboratory, Berkeley, California 94720*
[2]*Institute of Solid State Physics, Russian Academy of Sciences, 142432 Chernogolovka, Russia*
[3]*Department of Electrical and Computer Engineering,*
University of California, Santa Barbara, CA 93106
[4]*Department of Physics, University of California at Berkeley, Berkeley, California 94720*

Macroscopically ordered arrays of vortices in quantum liquids, such as superconductors, He–II, and atom Bose–Einstein Condensates (BEC), demonstrate macroscopic coherence in flowing superfluids [1, 2, 3, 4]. Despite of the rich variety of systems where quantum liquids reveal macroscopic ordering, experimental observation of a macroscopically ordered electronic state in semiconductors has remained a challenging unexplored problem. A system of excitons is a promising candidate for the realization of macroscopic ordering in a quantum liquid in semiconductors. An exciton is a bound pair of an electron and a hole. At low densities, it is a Bose quasiparticle. At low temperatures, of the order of a few Kelvins, excitons can form a quantum liquid, i.e., a statistically degenerate Bose gas and eventually BEC [5, 6, 7, 8, 9]. Here, we report the experimental observation of a macroscopically ordered state in an exciton system.

We studied spatially resolved photoluminescence, PL, of quasi-two-dimensional gases of indirect excitons in $GaAs/Al_xGa_{1-x}As$ coupled quantum wells, QWs (Fig. 1b). Previous studies [7, 8, 9] have shown that coupled QWs is a unique system where a cold exciton gas, and, more generally, a cold gas of light boson quasiparticles, can be created. The indirect excitons in coupled QWs are characterized by high cooling rates, three orders of magnitude higher than in bulk GaAs, and long lifetime against electron–hole recombination, more than three orders of magnitude longer than in a single GaAs QW. This lifetime is much longer than the characteristic time scale for cooling of initially hot photogenerated excitons down to temperatures well below 1K, where the dilute quasi–two-dimensional Bose gas of indirect excitons becomes statistically degenerate [8]. Because the exciton mass, M, is small, even smaller than the free electron mass m_0, the quantum degeneracy temperature $T_0 = (\pi\hbar^2 n)/(2Mgk_B)$ (g is the spin degeneracy of the exciton state and k_B is the Boltzmann constant) exceeds 1 K at experimentally accessible exciton densities, n, i.e. is several orders of magnitude higher than for atoms.

Yet another important advantage of the system is a repulsive interaction between the indirect excitons which, because of the separation of the electron and hole layers (Fig. 1b), are dipoles oriented perpendicular to the QW plane. This dipole-dipole interaction stabilizes the exciton state against the formation of metallic electron-hole

droplets in real space [10, 11], reinforces BEC [12], and results in a screening of an in-plane random potential (caused by interface fluctuations, impurities, etc. and unavoidable in any real QW sample). Note, that in ideal two-dimensional systems pure BEC is only possible at $T = 0$, although, a phase transition to a superfluid exciton state is possible at finite temperatures [13]. The latter is characterized by a long-range order at low temperatures [14].

Typically, excitons in semiconductors are generated by a laser photoexcitation and their density is controlled by the laser intensity. The indirect excitons have a small oscillator strength because of the small overlap between electron and hole wavefunctions. Therefore, a much higher density of indirect excitons is achieved by nonresonant laser photoexcitation with energies at or above the direct exciton resonance where the photon absorption coefficient is high (Fig. 1b). In a quasiequilibrium, practically all photoexcited carriers relax to the indirect exciton states as they are lower in energy than the direct exciton states (the ratio between the indirect and direct exciton densities is typically larger than 10^4). The cost to pay for the nonresonant excitation is that the initially photogenerated excitons are hot. However, they quickly cool down to the lattice temperature via phonon emission: e.g. the exciton temperature can drop down to 400 mK in about 5 ns, that is the time much shorter than the indirect exciton lifetime [8]. Therefore, there are two ways to overcome the obstacle of hot generation and study cold gases of indirect excitons with effective temperatures close to that of the lattice: (1) use a discrimination in time and study the indirect excitons a few ns after the end of the photoexcitation pulses [8], (2) use a discrimination in space and study the indirect excitons beyond the photoexcitation spot. In the latter case, excitons can cool down to the lattice temperature as they travel away from photoexcitation spot.

Here, exploring the spatially and spectrally resolved PL experiments, we have observed a ring structure in the indirect exciton photoluminescence and a macroscopically ordered state of indirect excitons appearing in the ring the most remote from the excitation spot. First we present a brief description of our experimental findings, that is followed by a discussion of the observed effects.

At the lowest excitation powers, P_{ex}, the spatial profile of the indirect exciton PL intensity practically follows the laser excitation intensity (Fig. 1a). However, at high P_{ex}, we observed a nontrivial pattern for that profile. First,

FIG. 1: Radial dependence of the indirect exciton PL. **a**, Peak intensity of the indirect exciton PL vs r, the distance from the excitation spot center, at $T = 1.8$ K, $V_g = 1.22$ V, and the excitation powers $P_{ex} = 6, 33, 95, 220, 290, 390, 530$, and 770 μW. **c**, Peak intensity of the indirect exciton PL vs r at $P_{ex} = 390$ μW, $V_g = 1.22$ V, and $T = 2.4, 4.4, 7, 10$, and 14 K. For comparison, the solid line shows the peak intensity variation of the direct exciton PL. The excitation spot profiles are shown by the dotted lines in **a** and **c**. The corresponding spatial dependence of the PL spectra at $T = 2.4$ and 14 K are shown in **e** and **f**. The upper spectra correspond to the excitation spot center, the lowest spectra are recorded 107μm away from the excitation spot center, and the step is 3.7μm. The indirect exciton PL line is at $\approx 1.545 - 1.55$ eV, the direct PL line is at ≈ 1.57 eV, the broad line arising below the indirect exciton emission comes from the bulk $n^+ -$GaAs emission. The selected spectra at $T = 2.4$ K are shown in (**d**): the spectrum in the excitation spot center at $r = 0$ (red), the spectrum in the first ring center at $r = 29\mu$m (green), and the spectrum in the second ring center at $r = 83\mu$m (black, the spectrum intensity is multiplied by 4). **b**, Energy band diagram of the CQW structures. The PL of indirect excitons is characterized by the rings centered at the excitation spot: the internal ring is located near the edge of the excitation spot, while the external ring is observed far away from the excitation spot.

we address its radial dependence detailed in Fig. 1. The pattern is characterized by a ring structure: the laser excitation spot is surrounded by two concentric bright rings separated by an annular dark interring region (the ratio between the indirect exciton PL intensities in the external ring and in the dark interring region reaches a factor of 30 at high P_{ex}). The rest of the sample outside the external ring is dark. The internal ring appears near the edge of the laser excitation spot, and the external ring can be remote from the excitation spot by more than 100 μm. Its radius increases with increasing excitation power. The ring structure follows the laser excitation spot when it is moved over the whole sample area. This nontrivial spatial profile of the indirect exciton PL intensity is only observed at low temperatures. When the temperature is increased the bright rings wash out, the PL intensity in the interring region and outside the external ring increases, and the spatial profile intensity approaches a monotonic bell-like shape (Fig. 1c).

The azimuthal dependence of the indirect exciton PL intensity in the external ring is also nontrivial: that ring is fragmented into circular-shape structures that form a periodic array, Figs. 2a–e. These fragments follow the external ring either when the excitation spot is moved over the sample area or when the ring radius varies with P_{ex}. The bright fragments always keep the circular shape with equal dimensions in radial and azimuthal directions under all experimental conditions studied. As already mentioned, they form a nearly periodic chain over macroscopic lengths, up to ~ 1 mm. This is demonstrated in Fig. 3e which shows the nearly linear dependence of the fragment positions along the ring vs their number. Along the whole external ring, both in the peaks and the passes, the indirect exciton PL lines are spectrally narrow with the full width at half maximum, FWHM, ≈ 1.3 meV, considerably smaller than in the center of the excitation spot, Figs. 2f and 1d. The ring fragmentation is observed at the lowest temperatures only and is already absent at $T \approx 4$ K, Figs. 3a-c. The PL contrast along the ring washes out as the temperature increases, this can be quantified by the amplitude of the Fourier transform of the variation of the PL intensity along the ring as shown in Fig. 3d.

Besides the mobile features, like the rings and the external ring's fragments that move with the excitation spot or when P_{ex} is varied, the spatial pattern shows also that the indirect exciton PL intensity is strongly enhanced in certain fixed spots on the sample, Figs. 2a–e. We call them localized bright spots (LBS). For any excitation spot location and any P_{ex} the LBS are only observed when they are within the area terminated by the external ring, Figs. 2a–e. In the LBS the indirect exciton PL line is spectrally narrow, FWHM ≈ 1.2 meV, and its energy is locally reduced. The LBS also wash out with increasing temperature.

All these effects are observed on several mesas studied and all experimental data are reproducible after cycling the sample temperature up to room temperature

FIG. 3: Temperature dependence of the spatial pattern of the indirect exciton PL intensity. **a, b**, The pattern at $T = 1.8$ (**a**) and 4.7 K (**b**) for $V_g = 1.22$ V, and $P_{ex} = 690\mu$W. The area of view is $475 \times 414\mu$m. **c**, The corresponding variation of the indirect exciton PL intensity along the external ring at $T = 1.8, 4.7,$ and 7.7 K. The ring fragmentation into the periodic chain washes out with increasing temperature. This is visualized by the PL contrast (**d**) presented by an amplitude of the Fourier transform. The dependence of the position of the indirect exciton PL intensity peaks along the external ring vs the peak number is nearly linear (**e**), showing that the fragments form a periodic chain.

Those are the states with small in-plane center of mass momenta $K_\parallel \leq K_0 = E_g\sqrt{\varepsilon}/(\hbar c)$ (E_g is the band gap and ε is the dielectric constant). The exciton radiative decay rate and, therefore, the exciton PL intensity are determined by the fraction of excitons inside the radiative zone. In the center of the excitation spot the exciton gas is characterized by a high effective temperature, larger than that of the lattice [8]. Under cw photoexcitation, there is a continuous flow of excitons out of the excitation spot due to the exciton drift and diffusion (other mechanisms such as ballistic transport and phonon wind may also be contributing to the exciton cloud expansion). The exciton diffusion originates directly from the exciton density gradient. The exciton drift also originates from the density gradient as the latter gives rise to the gradient of the indirect exciton energy because of the repulsive interaction (see Figs. 1e, f). As the excitons travel away from the excitation spot, the effective exciton tempera-
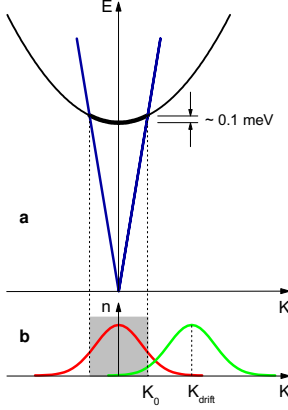
FIG. 4: Schematics demonstrating a reduction of emission intensity for excitons in motion. **a**, Energy diagram for the exciton and photon dispersion, the bold sector of the exciton dispersion indicates the radiative zone. **b**, The schematic momentum distribution of excitons without (red) and with (green) average drift velocity. The exciton radiative decay rate is proportional to the fraction of excitons in the radiative zone (grey area).

ture, T_X, decreases with increasing the radial distance due to their energy relaxation. The reduction of T_X increases the radiative zone occupation and, therefore, increases the PL intensity, that is seen as onset of the internal ring. The internal ring is therefore the spatial analog of the PL intensity enhancement after an excitation pulse, i.e. the PL jump, observed in Ref. [8]. Estimates for the exciton density in the internal ring exceed 3×10^{10} cm^{-2} at the highest P_{ex}, implying that a statistically degenerate Bose gas of indirect excitons forms in the internal ring (at $n = 3 \times 10^{10}$ cm^{-2} and $T = 2$ K, the Bose-Einstein distribution function gives the occupation number of the lowest energy state $\nu = e^{T_0/T} - 1 \approx 0.3$ for the excitons in our coupled QWs where $g = 4$ and $M = 0.21 m_0$).

To explain the dark region between the rings we propose the following scenario (Fig. 4). Travelling out of the energy "hill" at the center of the excitation spot excitons acquire an average drift momentum. As the height of the energy hill, several meV (Fig. 1e), is much larger than the radiative zone energy width, ~ 0.1 meV, the average momentum acquired, K_{drift}, can exceed K_0. That means that the moving excitons move out of the radiative zone and, therefore, become optically inactive. This explains the existence of the dark region between the internal and external rings. An interesting aspect of this effect is that the optically inactive excitons move at speeds several times faster than the speed of sound: already for $K = K_0$ excitons their speed $v = \hbar K_0/M = 1.4 \times 10^6$ cm/s is larger than the speed of sound in GaAs $v_s = 3.7 \times 10^5$

cm/s. This implies that the exciton flow in the dark interring region is diffusive rather than superfluid, because the Landau criterion for superfluidity is not fulfilled for excitons moving with supersonic velocities (the exciton moving with $v \geq v_s$ can scatter to a lower energy state with an acoustic phonon emission, and this process causes a dissipation). Far from the excitation spot the main driving force for exciton transport, the energy gradient, vanishes and they relax down to the lowest energy states. This results in the sharp enhancement of the radiative zone occupation and, therefore, the PL intensity, that is seen as the external ring. As excitons in the external ring relax down to the low momentum states, characterized by low velocities, the exciton flow is stopped and there are practically no excitons outside of that ring (Figs. 2a–e).

The most interesting feature of the external ring is its fragmentation into a periodic array. The existence of this periodic ordering shows that the exciton state formed in the external ring has a coherence on a macroscopic length scale. We emphasize that the coherence is not driven by a laser excitation because in our experiment the photoexcited carriers experience multiple inelastic scatterings before the optically active indirect excitons are formed. Instead, the coherence spontaneously appears in the exciton system. The understanding of the microscopic nature of this ordered exciton state warrants future studies. We suggest that the fragments are vortices in the exciton system and that the ordering is the consequence of a repulsive interaction between the vortices. This is confirmed by the fact that the fragments are always of a circular shape. The vortex rotation is continuously supported by the exciton flow out of the excitation spot. Similar to arrays of vortices in atom BEC [4], the rotation can be initiated even without an apparent external torque. A possible cause for the initiation of the rotation is a small deviation from axial symmetry for the exciton flow due to the in-plane potential fluctuations, which could result in a branching of the exciton flow, e.g. similar to the branching observed for the electron flow [16]. We note also that a spontaneous macroscopic flow organization with periodic vortical structures is a general property of thermodynamically open systems described by nonlinear partial differential equations [1, 2, 3, 4, 17].

In-plane potential fluctuations could influence also position of the vortices on the external ring due to the pinning effect. However, the pinning effect appears to be small so that vortices remain free to move (e.g. with changing of the excitation spot location on the sample) and the deviation of the vortex position out of the periodic array due to the pinning force is small (Fig. 3e). On the contrary, potential fluctuations can play a crucial role in formation of the LBS observed inside the external ring. Based on the current data, we suggest that in the LBS the optically inactive moving indirect excitons are captured by a potential trap formed by in-plane potential fluctuations, relax to the optically active exciton states, and recombine giving rise to the spectrally narrow emission seen as the LBS. The LBS will be studied

in details later. In the context of the model discussed here, we note: (i) the existence of LBS in the dark annular region between the two rings confirms the presence of the optically inactive excitons in this region and (ii) the absence of LBS outside of the external ring confirms the absence of excitons there.

Note that the spatial profiles of the direct exciton PL intensity exhibit none of the above effects and practically follows the laser excitation profile for all temperatures and excitation densities studied, Fig. 1c (this is also the case for the bulk GaAs emission). This is consistent with a short lifetime of direct excitons that limits the distance they can travel before the recombination and does not allow an effective cooling for them.

Methods

n^+-i-n^+ GaAs/AlGaAs CQW structure was grown by MBE. The i-region consists of two 8nm GaAs QWs separated by a 4nm $Al_{0.33}Ga_{0.67}As$ barrier and surrounded by two 200nm $Al_{0.33}Ga_{0.67}As$ barrier layers. The electric field in the sample growth direction is monitored by the external gate voltage V_g applied between the highly conducting n^+-layers. The narrow PL linewidth indicates a small in-plane disorder. For $V_g \approx 0$ the ground state of the optically pumped CQW is the direct exciton made of electron and hole in the same layer and similar to the excitons in single QWs. For nonzero V_g the ground state is the indirect exciton made of electrons and holes in different layers, Fig. 1b. The indirect exciton lifetime is in the range of tens and hundreds of ns. The indirect exciton energy shift with density, $\delta E(n)$, allows us to evaluate their concentration using $\delta E(n) = 4\pi ne^2 d/\varepsilon$, where d is the effective separation between the electron and hole layers. Radiative recombination is the dominant decay mechanism of indirect excitons in our high-quality sample. The sample was excited with a HeNe laser, $\lambda = 632.8$nm. The experiments were performed in He^4 cryostat with optical windows. Spatially resolved PL spectra were detected using a pinhole in the intermediate image plane. In the image experiment, the spatial pattern of the indirect exciton PL intensity was detected by CCD camera using spectral selection of the indirect exciton emission by the interference filter adjusted to the indirect exciton energy. The spatial resolution was 5μm.

[1] Essmann, U. & Träuble, H. The direct observation of individual flux lines in type II superconductors, *Phys. Lett.* **24A** 526-527 (1967).

[2] Yarmchuk, E.J., Gordon, M.J.V., & Packard, R.E. Observation of stationary vortex arrays in rotating superfluid helium, *Phys. Rev. Lett.* **43**, 214-217 (1979).

[3] Madison, K.W., Chevy, F., Wohlleben, W., and & Dalibard, J. Vortex formation is stirred Bose-Einstein condensate, *Phys. Rev. Lett.* **84**, 806-809 (2000).

[4] Abo-Shaeer, J.R., Raman, C., Vogels, J.M., & Ketterle, W. Observation of vortex lattices in Bose-Einstein Condensates, *Science* **292**, 476-479 (2001).

[5] Keldysh, L.V. & Kozlov, A.N. Collective properties of excitons in semiconductors. *Zhurnal Eksperimental'noi i Teoreticheskoi Fiziki* **54**, 978-993 (1968) [*Sov. Phys. JETP* **27**, 521-528 (1968)].

[6] Lozovik, Yu.E. & Yudson, V.I. A new mechanism for superconductivity: pairing between spatially separated electrons and holes, *Zhurnal Eksperimental'noi i Teoreticheskoi Fiziki* **71**, 738-753 (1976) [*Sov. Phys. JETP* **44**, 389-397 (1976)].

[7] Butov, L.V. & Filin, A.I. Anomalous transport and luminescence of indirect excitons in AlAs/GaAs coupled quantum wells as evidence for exciton condensation. *Phys. Rev. B* **58**, 1980-2000 (1998).

[8] Butov, L.V., Ivanov, A.L., Imamoglu, A., Littlewood, P.B., Shashkin, A.A., Dolgopolov, V.T., Campman, K.L., & Gossard, A.C. Stimulated scattering of indirect excitons in coupled quantum wells: Signature of a degenerate Bose-gas of excitons. *Phys. Rev. Lett.* **86**, 5608-5611 (2001).

[9] Butov, L.V., Lai, C. W., Ivanov, A.L., Gossard, A. C., & Chemla D. S. Towards Bose-Einstein condensation of excitons in potential traps. *Nature (London)*, scheduled for publication in May 2, 2002 issue.

[10] Yoshioka, D. & MacDonald, A.H. Double quantum well electron-hole systems in strong magnetic fields, *J. Phys. Soc. Jpn.* **59**, 4211 (1990).

[11] Zhu, X., Littlewood, P.B., Hybertsen, M. & Rice, T. Exciton condensate in semiconductor quantum well structures. *Phys. Rev. Lett.* **74**, 1633-1636 (1995).

[12] Leggett, A.J. Bose-Einstein condensation in the alkali gases: Some fundamental concepts. *Rev. Mod. Phys.* **73**, 307-356 (2001).

[13] Popov, V.N. On the theory of the superfluidity of two- and one-dimensional Bose systems. *Theor. Math. Phys.* **11**, 565-573 (1972).

[14] Kosterlitz, J.M. & Thouless, D.J. Ordering, metastability and phase transitions in two-dimensional systems, *J. Phys. C* **6**, 1181-1203 (1973).

[15] Feldmann, J., Peter, G., Göbel, E.O., Dawson, P., Moore, K., Foxon, C., and Elliott, R.J. Linewidth dependence of radiative exciton lifetimes in quantum wells. *Phys. Rev. Lett.* **59**, 2337 (1987).

[16] Topinka, M.A., Leroy, B.J., R. M. Westervelt, R.M., Shaw, S.E.J., Fleischmann, R., Heller, E.J, Maranowski, K.D., & Gossard, A.C., Coherent branched flow in a two-dimensional electron gas, *Nature (London)* **410**, 183 - 186 (2001).

[17] Taylor, G.I. Stability of a viscous liquid contained between two rotating cylinders, *Philos. Trans. R. Soc. London Ser. A* **223**, 289-343 (1923).